JBC RESEARCH ARTICLE

The vital hormone 20-hydroxyecdysone controls ATP production by upregulating binding of trehalase 1 with ATP synthase subunit α in *Helicoverpa armigera*

Received for publication, August 2, 2021, and in revised form, December 18, 2021 Published, Papers in Press, January 6, 2022,
https://doi.org/10.1016/j.jbc.2022.101565

Yanpeng Chang[‡], **Bo Zhang**[‡], **Mengfang Du, Zichen Geng, Jizhen Wei, Ruobing Guan, Shiheng An, and Wenli Zhao**[*]
From the State key Laboratory of Wheat and Maize Crop Science/College of Plant Protection, Henan Agricultural University, Zhengzhou, China

Edited by Henrik Dohlman

Trehalose is the major "blood sugar" of insects and it plays a crucial role in energy supply and as a stress protectant. The hydrolysis of trehalose occurs only under the enzymatic control of trehalase (Treh), which plays important roles in growth and development, energy supply, chitin biosynthesis, and abiotic stress responses. Previous reports have revealed that the vital hormone 20-hydroxyecdysone (20E) regulates Treh, but the detailed mechanism underlying 20E regulating Treh remains unclear. In this study, we investigated the function of HaTreh1 in *Helicoverpa armigera* larvae. The results showed that the transcript levels and enzymatic activity of HaTreh1 were elevated during molting and metamorphosis stages in the epidermis, midgut, and fat body, and that 20E upregulated the transcript levels of *HaTreh1* through the classical nuclear receptor complex *EcR-B1/USP1*. HaTreh1 is a mitochondria protein. We also found that knockdown of *HaTreh1* in the fifth- or sixth-instar larvae resulted in weight loss and increased mortality. Yeast two-hybrid, coimmunoprecipitation, and glutathione-*S*-transferase (GST) pull-down experiments demonstrated that HaTreh1 bound with ATP synthase subunit alpha (HaATPs-α) and that this binding increased under 20E treatment. In addition, 20E enhanced the transcript level of *HaATPs-α* and ATP content. Finally, the knockdown of *HaTreh1* or *HaATPs-α* decreased the induction effect of 20E on ATP content. Altogether, these findings demonstrate that 20E controls ATP production by up-regulating the binding of HaTreh1 to HaATPs-α in *H. armigera*.

Trehalose, a storage disaccharide (α-D-glucopyranosyl-α-D-glucopyranoside), is present in bacteria, yeasts, fungi, invertebrates, and plants (1, 2). As the major blood sugar of insects, trehalose is biosynthesized in the fat body from glucose originating from food digested in the midgut and then immediately transported to target tissues by hemolymph circulation (3). Trehalose is the energy source for all insect physical activities, including growth and flight (4). In addition, it protects biomacromolecules and stabilizes cell structure under high and low temperature, drought, and other stresses (5, 6). For example, in *Gomphocerus sibiricus*, trehalose accumulation enhances high-temperature (30 °C) resistance (7). Therefore, trehalose is an important survival strategy for insects.

In insects, the trehalose concentration varies from 5 to 50 mM based on developmental stage, nutritional status, and environmental conditions (6). The concentration of trehalose in insects is controlled by its biosynthesis and decomposition. The biosynthesis of trehalose is catalyzed by trehalose-6-phosphate synthase and trehalose-6-phosphate phosphatase (5). Trehalase (Treh) is the only enzyme that catalyzes the hydrolysis of trehalose to glucose.

Two distinct forms of Treh exist in insects, soluble Treh (Treh1) and membrane-bound Treh (Treh2), based on the transmembrane structure at the C-terminus. Soluble Treh localizes to the cytoplasm and hydrolyzes cytoplasmic trehalose to glucose; it has been purified from insect hemolymph, midgut goblet cells, and egg homogenate (8–10). Membrane-bound Treh, which hydrolyzes extracellular trehalose into glucose and then glucose is absorbed in the cell, is a cell-membrane protein present in the flight muscles, follicular cells, ovarian cells, spermatid, midgut, brain, and thoracic ganglia of insects (11–14). Adenosine triphosphate is generated *via* glycolysis and the tricarboxylic acid cycle. Trehalase activity is modulated by fluctuation of the trehalose concentration in hemolymph. Hormones, such as 20-hydroxyecdysone (20E), juvenile hormone, insulin, and diapause hormone, regulate Treh activity (15–19).

20-hydroxyecdysone initiates egg hatching, larvae molting during different instars, pupal metamorphosis from larva to pupae, and emergence molting from pupae to adult in complete-metamorphosis insects (20, 21). As a fat-soluble molecule, 20E diffuses freely into cells and binds to its nuclear receptor, ecdysone receptor (EcR). Ecdysone receptor interacts with ultraspiracle protein (USP) to form a heterodimeric transcription complex, EcR/USP (22). 20-hydroxyecdysone-EcR/USP binds to ecdysone response elements in promoters to initiate 20E-responsive early gene transcription (23, 24), which activates the expression of late genes, resulting in molting or metamorphosis (25). 20-hydroxyecdysone induces the disintegration of larval organs and the reconstruction of adult organs during molting and

[‡] These authors contributed equally to this work.
[*] For correspondence: Wenli Zhao, zhaowenli19900218@163.com.

metamorphosis (26). For instance, the midgut shrinks to the lumen and gradually separates from the newly formed midgut for subsequent apoptosis during metamorphosis. The old epidermis peels away, and new epidermis is formed during molting (27–29). The molting and metamorphosis induced by 20E are energy-intensive processes.

There is abundant evidence on the relationship between 20E and Treh1. Validamycin A (a Treh inhibitor) significantly decreases the activities of two Trehs in *Nilaparvata lugens*, resulting in molting failure, which is similar to 20E signal disruption (30). Injection of 20E into *Apolygus lucorum* larvae increases the transcription and enzymatic activity of Treh1 (31). In *Antheraea pernyi*, the transcription and enzymatic activity of ApTreh-1A also increases in response to 20E (32). Furthermore, RNAi data have demonstrated the function of *Treh1* in insects (33). Trehalase and chitin synthetase (CHS) are enzymes that catalyze the first and last steps of the biosynthesis of chitin, a vital component of epidermis (3). In *Spodoptera exigua*, knockdown of *SeTreh1* decreases *CHSA* expression and epidermis chitin content, resulting in molting failure and a 50% mortality rate (34). The ds*Treh1*-injected *N. lugens* shows abnormities in molting and wing, and mortality is increased *via* disruption of the biosynthesis and degradation of chitin (35). Trehalase affects chitin biosynthesis, but the cellular signaling pathways are unknown.

Mitochondria are energy factories, and ATP is the energy currency. Oxidative phosphorylation is the main pathway of ATP biosynthesis, the terminal reaction of which is catalyzed by F0F1-ATP synthase (36). In the oxidative catabolism of glucose, cytoplasmic glucose is converted to pyruvate by glycolysis and mitochondria pyruvate to acetyl-CoA under aerobic conditions; acetyl-CoA is oxidized and decomposed into water in the tricarboxylic acid cycle. Electrons are transferred from NADH dehydrogenase to cytochrome c oxidase *via* coenzyme Q, cytochrome bc1 complex, and cytochrome c. The proton gradient established across the inner mitochondrial membrane drives the flow of protons through ATP synthase (ATPs) and is accompanied by ATP biosynthesis. F0F1-ATP synthase is a multi-subunit enzyme that contains two rotary motors, F0 and F1 (37, 38). The core mammalian F0F1-ATP synthase F0 consists of subunits a–g, which are embedded in the membrane to transports protons, and soluble F1 comprises subunits α–ε as and catalyzes ATP production (39, 40). ATP synthase subunit alpha (ATPs-α) is crucial for *Trypanosoma brucei*. Knockdown of *ATPs-α* decreases growth rate, ATP hydrolysis, and ATP synthesis of *T. brucei* (41–43).

In this study, the function of HaTreh1 and its relationship with 20E, especially the increased binding between HaTreh1 and HaATPs-α caused by 20E treatment of *Helicoverpa armigera* larvae, were explored. The results showed that 20E stimulates Treh to ensure the supply of energy, including ATP, during molting and metamorphosis, and provide an in-depth mechanism of Treh1 in insects and the new targets for pest management.

Results

The transcript level and enzymatic activity of HaTreh1 were elevated during the molting and metamorphosis stages

qRT-PCR was performed to investigate the expression of *HaTreh1* in larvae from the fourth-instar to the prepupal stage. *HaTreh1* transcript was expressed in three tissues (epidermis, midgut, and fat body), and its level peaked at 6L-4 days (the fourth day of sixth-instar larvae) in epidermis and midgut and at 4L-M (the molting stage of fourth-instar larvae) and 5L-M (the molting stage of fifth-instar larvae) in the fat body (Fig. 1, *A*–*C*). HaTreh1 activity peaked at 4L-M (epidermis and fat body) and 6L-5 (midgut) (Fig. 1, *D*–*F*). The expression and activity changes of HaTreh1 were consistent with the fluctuation of the 20E titer in 4L-M, 5L-M, 6L-4, and 6L-5, suggesting a role for 20E in regulating the transcript level of *HaTreh1*.

20-hydroxyecdysone upregulated the transcript level of HaTreh1 *via* EcR-B1 *and* USP1

The transcript level of midgut *HaTreh1* was significantly increased by 20E after 6, 12, and 24 h compared with the dimethyl sulfoxide (DMSO)-injected control midguts, as shown by qRT-PCR (Fig. 2*A*). After knockdown of the 20E receptor complex *EcR-B1*/*USP1* in the midgut by dsRNA (Fig. 2, *B* and *C*), the increase in *HaTreh1* transcript induced by 20E was diminished in ds*EcR-B1*+20E-injected and ds*USP1*+20E-injected midguts compared with that in ds*GFP*+20E-injected midguts (Fig. 2*D*). These results suggested that 20E increased the transcript level of *HaTreh1 via* its receptors, *EcR-B1* and *USP1*.

Knockdown of HaTreh1 *caused weight loss and mortality in larvae*

In fifth-instar larvae, ds*HaTreh1*-injection caused a significant decrease in the *HaTreh1* transcript level, compared with the ds*GFP*-injected control (Fig. 3*A*). Also, ds*HaTreh1*-injection caused significant decreases in the size and weight of fifth-instar larvae, compared with those injected with ds*GFP*, at 24 and 48 h after injection (Fig. 3, *B* and *C*). Furthermore, the mortality rate was higher in ds*HaTreh1*-injected fifth-instar larvae than ds*GFP*-injected larvae (5.5% *versus* 1.1% at 24 h and 24.4% *versus* 6% at 48 h, respectively) (Fig. 3*D*).

In sixth-instar larvae, qRT-PCR showed that *HaTreh1* had no effect on the mRNA level of *HaTreh2* (Fig. 4*A*), suggesting successful and specific knockdown of *HaTreh1*. The size and weight of ds*HaTreh1*-injected sixth-instar larvae were significantly lower than those of ds*GFP*-injected larvae from 24 to 144 h after dsRNA injection (Fig. 4, *B* and *C*). The mortality rate of ds*HaTreh1*-injected sixth-instar larvae increased from 24 h reaching 93.1% at 144 h after ds*HaTreh1* injection, compared with 7.6% in the ds*GFP*-injected group (Fig. 4*D*). The ds*HaTreh1*-injected sixth-instar larvae died at the pupal or larval stage (Fig. 4*B*). Accordingly, these results suggest that *HaTreh1* knockdown caused weight loss and increased the mortality rate of fifth- and sixth-instar larvae.

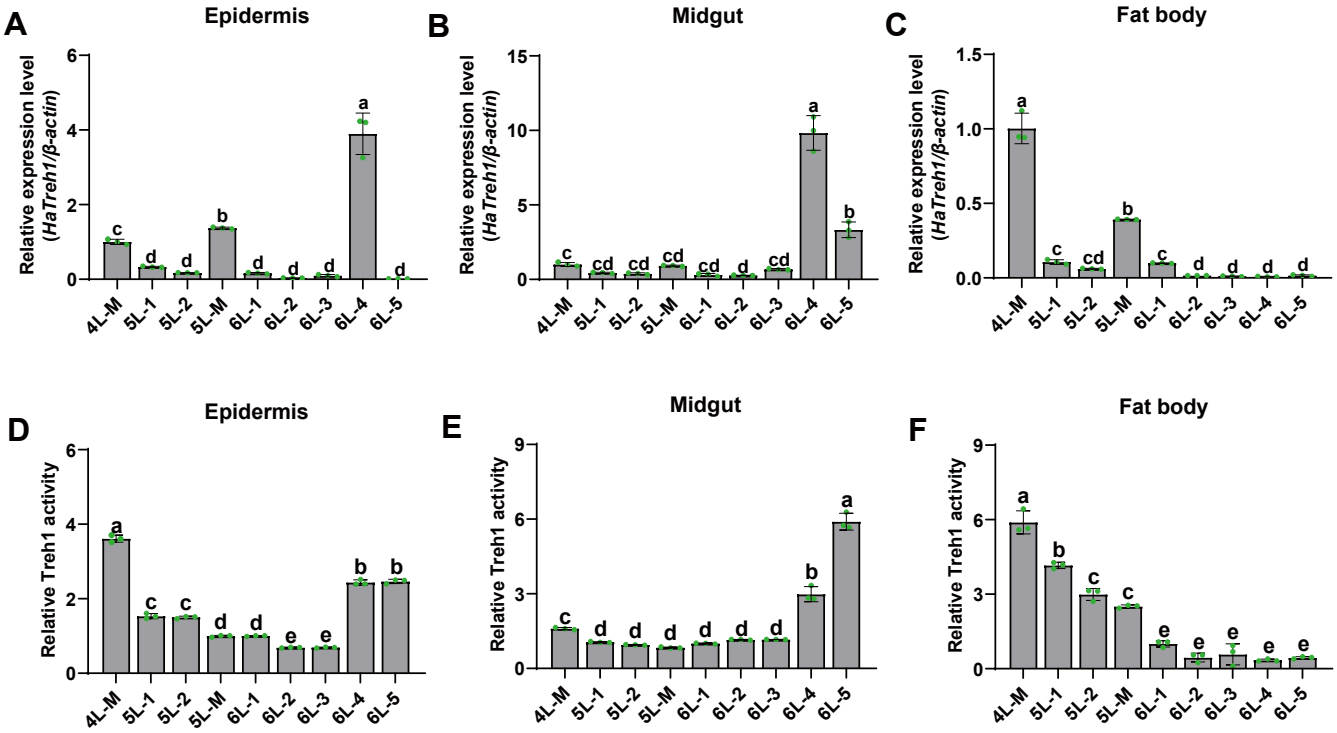

Figure 1. The expression and enzymatic activity of HaTreh1 in the larvae. *A–C*, the transcript levels of *HaTreh1* in epidermis (*A*), midgut (*B*), and fat body (*C*) by qRT-PCR. *β-actin* was used as the reference gene. The error bars indicated the mean ± s.d. of three independent biological experiments and three technical repetitions. *Different letters* indicate significant differences at $p < 0.05$ level by Tukey test. *D–F*, enzymatic activity of HaTreh1 in epidermis (*D*), midgut (*E*), and fat body (*F*). The error bars indicated the mean ± s.d. of three independent biological experiments and three technical repetitions. *Different letters* indicate significant differences at $p < 0.05$ level by Tukey test. 4L, the fourth-instar; 5L, the fifth-instar; 6L: the sixth-instar; M, molting; Treh1, soluble Treh.

HaTreh1 is a mitochondrial protein

The cytoplasmic localization of HaTreh1- Red fluorescent protein (RFP)-His protein was evaluated by fluorescence imaging and Western blotting. Red fluorescent protein-His (control) protein was localized to the cytoplasm and nucleus of midgut (MG) cells (Fig. 5, *A* and *B*). The red fluorescence of HaTreh1-RFP-His overlapped with the green fluorescence of Mito-tracker green in mitochondria (Fig. 5*C*), indicating mitochondrial localization of HaTreh1-RFP-His protein.

20-hydroxyecdysone increased the binding of HaTreh1 to HaATPs-α

Proteins interacting with HaTreh1 were identified by yeast two-hybrid (Y2H) library screening using HaTreh1-pGBKT7 as bait (Fig. S1). HaTreh1 with ATP synthase subunit alpha was found to bind to HaTreh1 in Y2H (point to point), glutathione-S-transferase (GST) pull-down and coimmunoprecipitation (Co-IP) assays. The Y2H assay showed that mating yeast cells containing BD-HaTreh1 and AD-HaATPs-α grew well on SD-TL, SD-THL, and SD-THLA plates and activated the expression of lacZ (Fig. 6*A*), similar to the positive control (BD-P53+AD-LargeT) and in contrast to the negative control (BD-laminC+AD-LargeT), suggesting that HaTreh1 and HaATPs-α interact. HaTreh1 with ATP synthase subunit alpha-GST protein pulls down HaTreh1-His protein but not the GST protein control (Figs. 6*B* and S2). The yellow fluorescence suggested the colocalization of HaTreh1-RFP-His with HaATPs-α-GFP-His (Figs. 6*C* and S3). Furthermore, Co-IP in MG cells and Sf9 cells overexpressing HaTreh1-RFP-His+HaATPs-α-GFP-His showed that 20E increased the binding of HaTreh1-RFP-His and HaATPs-α-GFP-His (Fig. 6, *D* and *E*). Therefore, 20E enhanced the interaction between HaTreh1 and HaATPs-α.

HaTreh1 and HaATPs-α affected the ATP content of larvae

Knockdown of *HaTreh1* resulted in a significant increase in trehalose content (Fig. 7*A*) and a significant decrease in glucose content (Fig. 7*B*). 20-hydroxyecdysone significantly increased the ATP content (Fig. 7*C*) and the transcript level of *HaATPs-α* in the midgut (Fig. 7*D*). Knockdown of *HaATPs-α* (Fig. S4) or *HaTreh1* significantly decreased the 20E-mediated increase in ATP content (Fig. 7*E*). These results suggest that 20E increases the ATP content in a manner dependent on HaTreh1 and HaATPs-α.

Discussion

The development of complete-metamorphosis insects is controlled by 20E and JH (20). There is a relationship between 20E and Treh; however, the in-depth mechanism is unknown. In this study, *H. armigera* larvae were used to investigate the role of Treh1 in larvae. The transcript level and enzymatic activity of HaTreh1 peaked during the

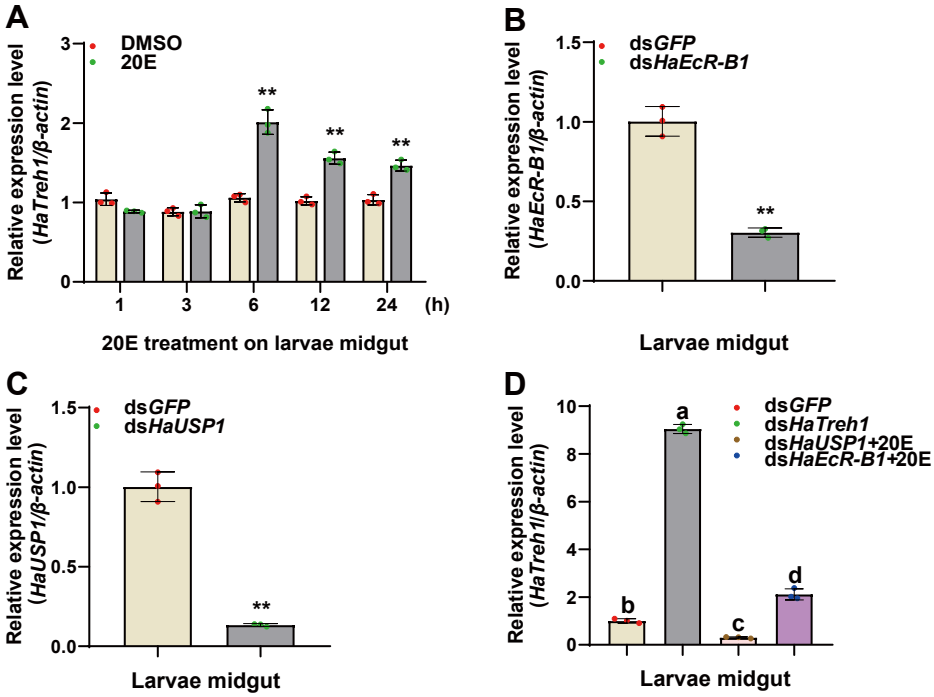

Figure 2. 20-hydroxyecdysone increased the transcript level of *HaTreh1 via* EcR-B1/USP1. *A*, the transcript level of midgut *HaTreh1* was upregulated under 20E treatment by qRT-PCR. The sixth-instar larvae were injected with 1.2 μg 20E (5 μl, 1 μM) or dimethyl sulfoxide (5 μl) for 1, 3, 6, 12, and 24 h. Then, midguts were collected for qRT-PCR. *β-actin* was used as the reference gene. The error bars indicated the mean ± s.d. of three independent biological experiments and three technical repetitions. $^{**}p < 0.01$, Student's *t* test. *B*, the knockdown effect of *HaUSP1* by qRT-PCR. The midguts of ds*HaUSP1* (5 μg)- or ds*GFP* (5 μg, control group)-injected sixth-instar larvae were collected at 24 h after injection. *β-actin* was used as the reference gene. The error bars indicated the mean ± s.d. of three independent biological experiments and three technical repetitions. $^{**}p < 0.01$, Student's *t* test. *C*, the knockdown effect of *HaEcR-B1* by qRT-PCR. The midguts of ds*HaEcR-B1* (5 μg)- or ds*GFP* (5 μg, control group)-injected sixth-instar larvae were collected at 24 h after injection. *β-actin* was used as the reference gene. The error bars indicated the mean ± s.d. of three independent biological experiments and three technical repetitions. $^{**}p < 0.01$, Student's *t* test. *D*, knockdown of *HaEcR-B1* or *HaUSP1* suppressed the induction effects of 20E on *HaTreh1* transcript levels by qRT-PCR. The 3 μg ds*EcR-B1*- or 3 μg ds*USP1*-injected sixth-instar larvae were injected with 5 μl 20E (1.2 μg, 1 μM) at 24 h after dsRNA injection, and then after 6 h, midguts were collected for qRT-PCR. ds*GFP* (3 μg)- or ds*GFP* (3 μg) + 5 μl 20E (1.2 μg)-injected larvae were used as the control groups. *β-actin* was used as the reference gene. The error bars indicated the mean ± s.d. of three independent biological experiments and three technical repetitions. *Different letters* indicate significant differences at $p < 0.05$ level by Tukey test. 20E, 20-hydroxyecdysone; EcR, ecdysone receptor; Treh1, soluble Treh; USP, ultraspiracle protein.

molting and metamorphosis stages, including at 4L-M, 5L-M, 6L-4, and 6L-5 days (Fig. 1). At 4L-M, 6L-4, and 6L-5 days, the newly formed midgut separates from the old midgut, a new epidermis forms, and the old epidermis molts (26). These stages require a considerable amount of a carbon source, such as glucose, a product of trehalose hydrolysis by Treh. Indeed, the expression and enzymatic activity of HaTreh1 were highly increased during these stages, in agreement with its function of supplying essential energy for cells. Trehalose is biosynthesized in the fat body and transported to target tissues by hemolymph circulation. Considering the huge energy demand at 6L-3 to 6L-5 days, the low transcript level and activity of HaTreh1 from 6L-2 to 6L-5 days in the fat body ensures that the trehalose in the fat body is not hydrolyzed (Fig. 1), thus maintaining a hemolymph level of trehalose sufficient to meet the energy needs of other tissues.

The upregulation of the *HaTreh1* transcript level by 20E was consistent with the peak of *HaTreh1* expression and high 20E titer during molting and metamorphosis (44). The increased transcript level of *Treh1* induced by 20E is not unique to *H. armigera*. 20-hydroxyecdysone also upregulates the transcript level of *AlTreh1* in *A. lucorum* (31), *ApTreh1-A* in *A. pernyi* (32), and *NlTreh1* in *N. lugens* (35). 20-hydroxyecdysone increased the transcript level of *HaTreh1 via* its receptor complex EcR-B1/USP1(Fig. 2), consistent with the findings in *A. pernyi*, in which the transcript level of *ApTreh1A* was downregulated after *ApEcRB1* knockdown or treatment with the EcR antagonist cucurbitacin B (32). However, the transcription factor initiating the transcription of *HaTreh1* under 20E treatment is unknown. Further study is needed to address the mechanism underlying the effect of 20E on *HaTreh1* transcription.

RNAi knockdown of *HaTreh1* in fifth- and sixth-instar larvae caused weight loss and increased the mortality rate (Figs. 3 and 4), consistent with the findings in other insects. For example, knockdown of *SeTreh-1* in *S. exigua* caused a mortality rate >50% (34). RNAi of two *Treh1s* resulted in abnormities in molting and wing development and increased mortality rate in *N. lugens* (30). RNAi of *Treh1-4* induced a mortality rate of >30% in *Tribolium castaneum* (45) and RNAi of *Treh1a* induced a mortality rate up to 80% in *Leptinotarsa decemlineata* (46). These results can be explained by the function of HaTreh1. Knockdown of *HaTreh1* caused

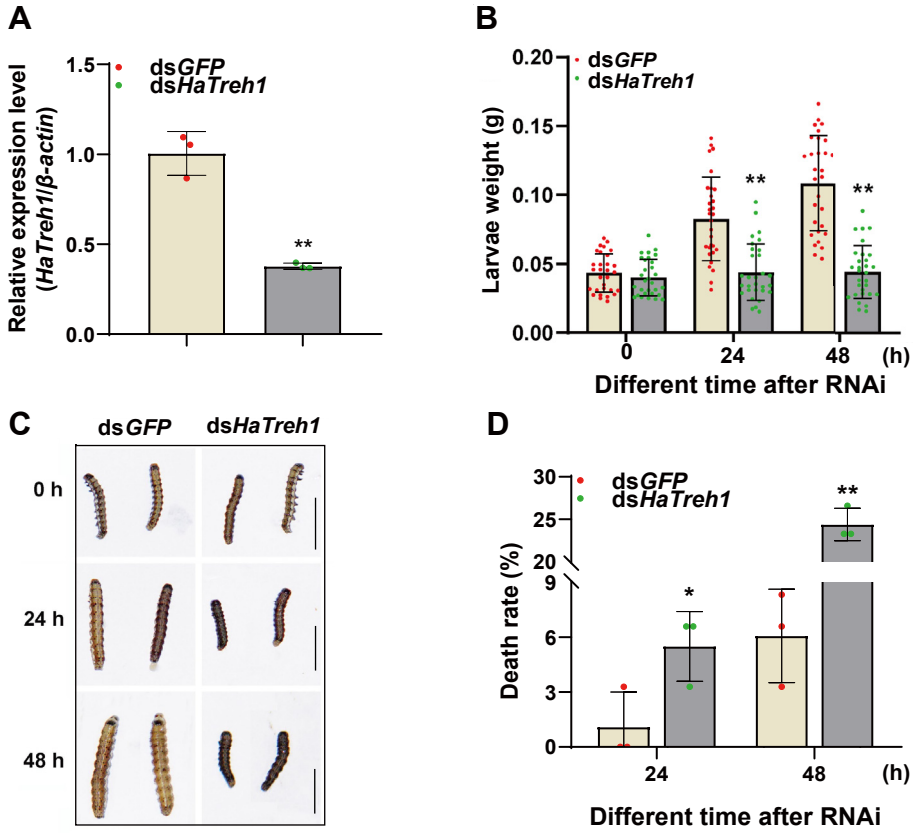

Figure 3. The effects of ds*HaTreh1*-injection on the fifth-instar larvae. *A*, knockdown effect of *HaTreh1* in the fifth-instar larvae midguts by qRT-PCR. Larvae were injected with ds*HaTreh1* (3 μg) or ds*GFP* (3 μg, control group) and 24 h later, midguts were collected. *β-actin* was used as the reference gene. The error bars indicated the mean ± s.d. of three independent biological experiments and three technical repetitions. $^{**}p < 0.01$, Student's *t* test. *B*, photos of fifth-instar larvae after injected with dsRNA for 24 h and 48 h. *C*, statistical analyses of larvae weight after injected with dsRNA for 24 h and 48 h. Thirty larvae in each group and three independent biological experiments were used. Each dot represented a repetition, the error bars indicate mean ± SE. $^{**}p < 0.01$ (Student's *t* test). The bars are 1 cm. *D*, statistical analyses of death rates after injected with dsRNA for 24 h and 48 h. Thirty larvae in each group. The error bars indicated the mean ± s.d. of three independent biological experiments and three technical repetitions. $^{*}p < 0.05$, $^{**}p < 0.01$, Student's *t* test. Treh1, soluble Treh.

accumulation of trehalose and a decrease in glucose content, leading to significant decreases in energy supply and chitin biosynthesis, ultimately causing the above mentioned phenotype.

Trehalase is localized to mitochondria in the flight muscle of blowfly (*Phormia regina*) (47) and flesh fly (*Sarcophaga bullata*) and in the thorax of the honeybee (48, 49). At present study, HaTreh1 is a mitochondrial protein (Figs. 5 and 6). And the colocalization, Y2H, GST pull-down, and Co-IP assays proved the interaction between HaTreh1 and HaATPs-α (Figs. 5 and 6). In *Locusta migratoria manilensis*, knockdown of *Lm-ATP5A* (ATPs-α) by dsRNA resulted in significant decreases in the survival rate of fifth-instar larvae and adults, as well as in ATPs activity and ATP content (50). This is in agreement with our finding in Treh-knockdown larvae, in which *HaTreh1* knockdown significantly decreased the ATP content, suggesting that HaATPs-α and HaTreh1 regulate ATP production (Fig. 7). Furthermore, 20E-mediated ATP production was dependent on HaATPs-α and HaTreh1. This binding of HaTreh1 to HaATPase-α is the first evidence for an interaction between Treh1 and ATPase-α.

20-hydroxyecdysone controls energy supply *via* Treh, as demonstrated by the decreased glucose content after knockdown of *HaTreh1* (Fig. 7). Furthermore, 20E enhances the binding of HaTreh1 to HaATPase-α to increase the ATP content, as evidenced by the decreased ATP content after knockdown of *HaTreh1*, *HaATPase-α*, or *HaTreh1+HaATPase-α* (Figs. 6 and 7). The interconnection of HaTreh1, HaATPase-α, and 20E with respect to ATP and glucose levels would explain the higher mortality upon *HaTreh1* knockdown, as energy supplies are then reduced. The biological relevance of HsTreh1 is, however, different to that reported for other insects; for instance, *SeTreh-1* of *S. exigua* (34), two *Treh1s* of *N. lugens* (30), and *Treh1-4* of *T. castaneum* (45) contribute only to CHS expression and the chitin content. Finally, we proposed the following functional model of HaTreh1 in *H. armigera* larvae: (1) 20-hydroxyecdysone upregulates the *HaTreh1* transcript level *via* EcR-B1/USP1 in the nucleus, (2) 20-hydroxyecdysone increases the glucose content *via* HaTreh1, and (3) 20-hydroxyecdysone increases ATP production by enhancing the binding of HaTreh1 and HaATPs-α in mitochondria, promoting the development of larvae (Fig. 8). Endogenous trehalase does not exist in mammals, and the biosynthesis and metabolism of disaccharides are different between mammals and insects. Studies on the molecular mechanism

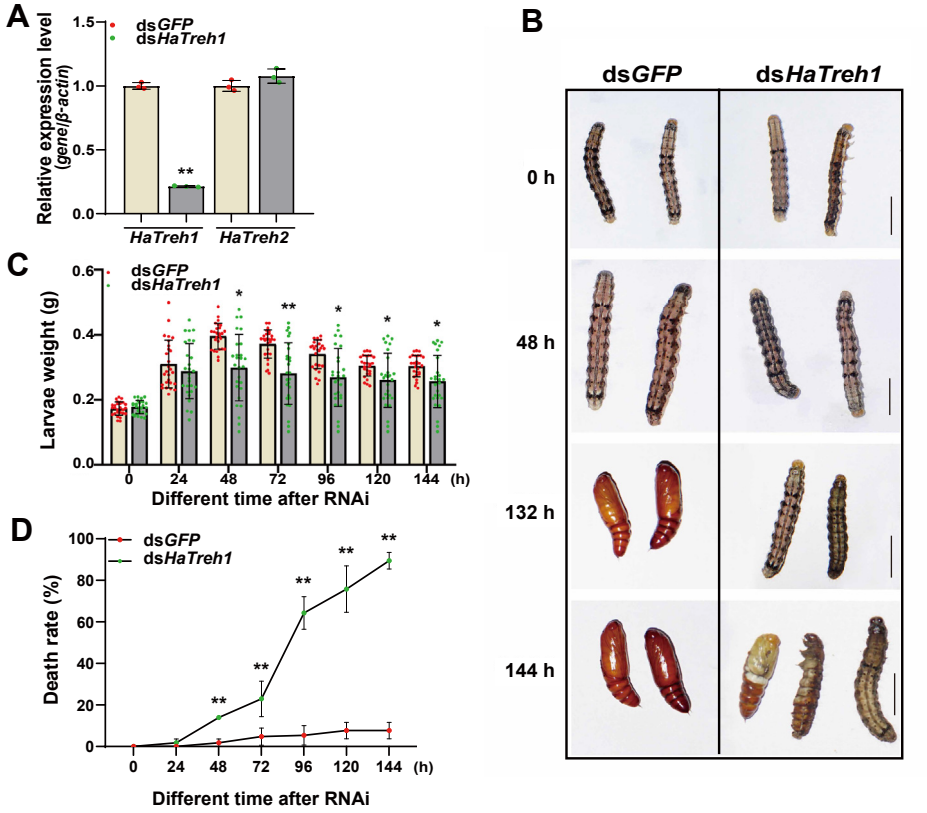

Figure 4. The effects ds*HaTreh1*-injection on the sixth-instar larvae. *A*, the specific knockdown effect of *HaTreh1* on the sixth-instar larvae midguts by qRT-PCR. Larvae were injected with ds*HaTreh1* (5 μg) or ds*GFP* (5 μg, control group), and midguts were collected at 24 h after dsRNA injection. *β-actin* was used as the reference gene. The error bars indicated the mean ± s.d. of three independent biological experiments and three technical repetitions. $^{**}p <$ 0.01, Student's *t* test. *B*, photos of sixth-instar larvae after injected with dsRNA for 48 h, 132 h, and 144 h. *C*, statistical analyses of larvae weight after injected with dsRNA for 24, 48, 72, 96, 120, and 144 h. Thirty larvae in each group and three independent biological experiments were used. Each dot represented a repetition, the error bars indicate mean ± SE. $^{*}p < 0.05$, $^{**}p < 0.01$, Student's *t* test. The bars are 1 cm. *D*, statistical analyses of death rates after injected with dsRNA for 24, 48, 72, 96, 120, and 144 h. Thirty larvae in each group. The error bars indicated the mean ± s.d. of three independent biological experiments. $^{**}p < 0.01$, Student's *t* test. Treh1, soluble Treh.

of HaTreh1 would facilitate the development of insecticides targeting Treh. Trehalase-targetting pesticides are nontoxic and have a less negative effect on animals (51).

Experimental procedures

Insects

Helicoverpa armigera larvae were reared with artificial medium and under 26 °C, 75% humidity, and 14L:10D photoperiod conditions (52).

Cell culture

Heliothis zea MG cells line is maintained at 28 °C and cultured with EX-Cell420 Serum-Free Medium (Sigma-Aldrich) that containing 10% fetal bovine serum and 0.5% Penicillin-Streptomycin Liquid as description in previous paper (53). *Spodoptera frugiperda* ovary cell line (Sf9 cells) was cultured with Sf-900 II Serum-Free Medium (containing 10% fetal bovine serum, 0.5% Penicillin-Streptomycin Liquid) at 28 °C. Fetal bovine serum (Gibco). Penicillin-Streptomycin Liquid (HyClone).

Chemicals

Ecdysterone was from Solarbio (Solarbio) and dissolved with DMSO.

qRT-PCR

The total RNA was extracted by the Trizol method and then reverse transcribed into cDNA by the Hiscript III RT SuperMix for qPCR (+gDNA wiper) (R323–01) (Vazyme) as the qRT-PCR template. The qRT-PCR reaction was performed on by using the ChamQ Universal SYBR qPCR Master Mix (Q711-02-03) (Vazyme) and a real-time qPCR instrument (Eppendorf). The qRT-PCR system containing 10 μl 2× ChamQ Universal SYBR qPCR Master Mix, 0.4 μl forward primer, 0.4 μl reverse primer, 1 μl cDNA template, and 8.2 μl ddH_2O. The corresponding reaction program was as follows: 95 °C (5 min), followed by 40 cycles of 95 °C (15 s) and 60 °C (20 s). The data was analyzed using the formula: $R = 2^{-[\Delta Ctsample-\Delta Ctcontrol]}$, where R referred to the relative expression level, the ΔCt sample was the difference

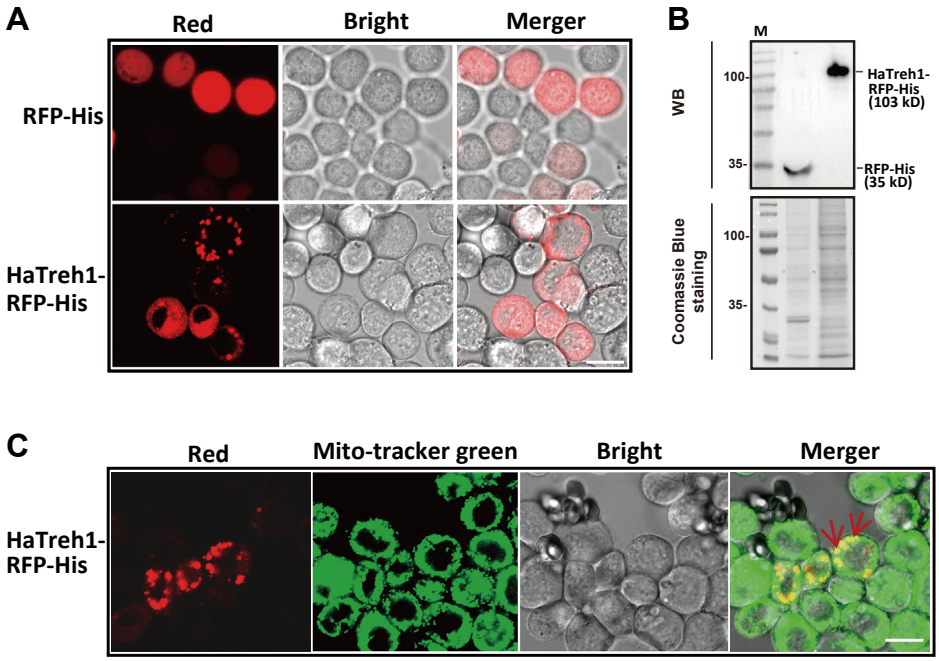

Figure 5. HaTreh1 is a mitochondrial protein. *A*, the fluorescence images of RFP-His and HaTreh1-RFP-His in midgut cells by LSM710 confocal microscope. The bar was 10 μm. Red fluorescent protein-His was the control. Merger was the overlap of Red and Bright. *B*, Western blot and Coomassie blue staining results of midgut cells overexpressing RFP-His (35 kD) or HaTreh1-RFP-His (101 kD). M: protein marker. *C*, the fluorescence of HaTreh1-RFP-His merged with mitochondria (dyed with mito-tracker, 50 nM, 15 min) green by LSM710. The bar was 10 μm. Merger was the overlap of *red*, mito-Tracker *green*, and *bright*. The *arrow* indicates the overlapped *yellow*. RFP, red fluorescent protein; Treh1, soluble Treh.

between the gene Ct value and the *β-actin* (Genbank NO. HM629442.1) Ct value in the experimental group (54), and ΔCt control was the difference between the gene Ct value and the *β-Actin* Ct value in the control group. Three biological replicates and three technical replicates were used for each experiment. The Student's *t* test or Turkey test were used to compare the significant differences.

20-hydroxyecdysone treatment on larvae

The sixth-instar larvae at 2 h after molting were injected with 5 μl 20E (1.2 μg, 1 μM). And the injection site was pleopod. Then, the midguts were collected at 1, 3, 6, 12, and 24 h after injection. Larvae injected with 5 μl DMSO (diluted to 1:10,000 with 1× PBS) were used as the control. The experiments were performed with three biological replicates and six larvae per group.

Double-stranded RNA synthesis

The DNA templates for ds*HaTreh1* (607 bp), ds*HaATPs-α* (484 bp), ds*HaEcR-B1* (348 bp), or *HaUSP1* (546 bp) synthesis were amplified by PCR with specific primers containing T7 promoter sequence (Table S1) and then subjected for *in vitro* dsRNA synthesis. The dsRNA was synthesized by the MEGAscript RNAi kit (ThermoFisher Scientific) according to the instruction description (55). The quality of dsRNA was detected by biophotometer (Eppendorf) and agarose electrophoresis. The dsRNA of GFP was used as the negative control (Genbank accession number MN623123, 422 bp).

Knockdown genes in larvae by RNAi

Knockdown of HaTreh1 *in the fifth-instar larvae*

The fifth-instar larvae at 2 h after molting were selected. The treated larvae were collected for qRT-PCR, phenotype photos, weight, and death rate analyses at 0, 24, and 48 h after ds*HaTreh1* injection (3 μg, 3 μl). The ds*GFP*-injected (3 μg, 3 μl) larvae were used as the control. Thirty larvae per group and three biological replicates were performed.

Knockdown of HaTreh1 *in the sixth-instar larvae*

The sixth-instar larvae at 2 h after molting were selected. Larvae were injected with 5 μg ds*HaTreh1* or 5 μg ds*EGFP* (5 μl). Phenotypes, weight, and death rates were recorded at 0, 24, 48, 72, 96, 120, and 144 h after dsRNA injection. Thirty larvae per group and three biological replicates were performed.

Knockdown of HaATPs-α *in the sixth-instar larvae*

The sixth-instar larvae at 2 h after molting were selected. The larvae were injected with 3 μg ds*HaATPs-α* or 3 μg ds*GFP* (3 μl). The midguts were collected for qRT-PCR and ATP content measurement at 24 h after dsRNA injection. Six larvae per group and three biological replicates were performed.

Knockdown of HaEcR-B1 *or* HaUSP1 *in the sixth-instar larvae*

The sixth-instar larvae at 2 h after molting were selected. The larvae were injected with 3 μg ds*EcR-B1* or 3 μg ds*USP1* (3 μl) and 24 h later, they were injected with 5 μl 20E (1.2 μg, 1 μM), after 6 h, midguts were collected for analysis. Larvae

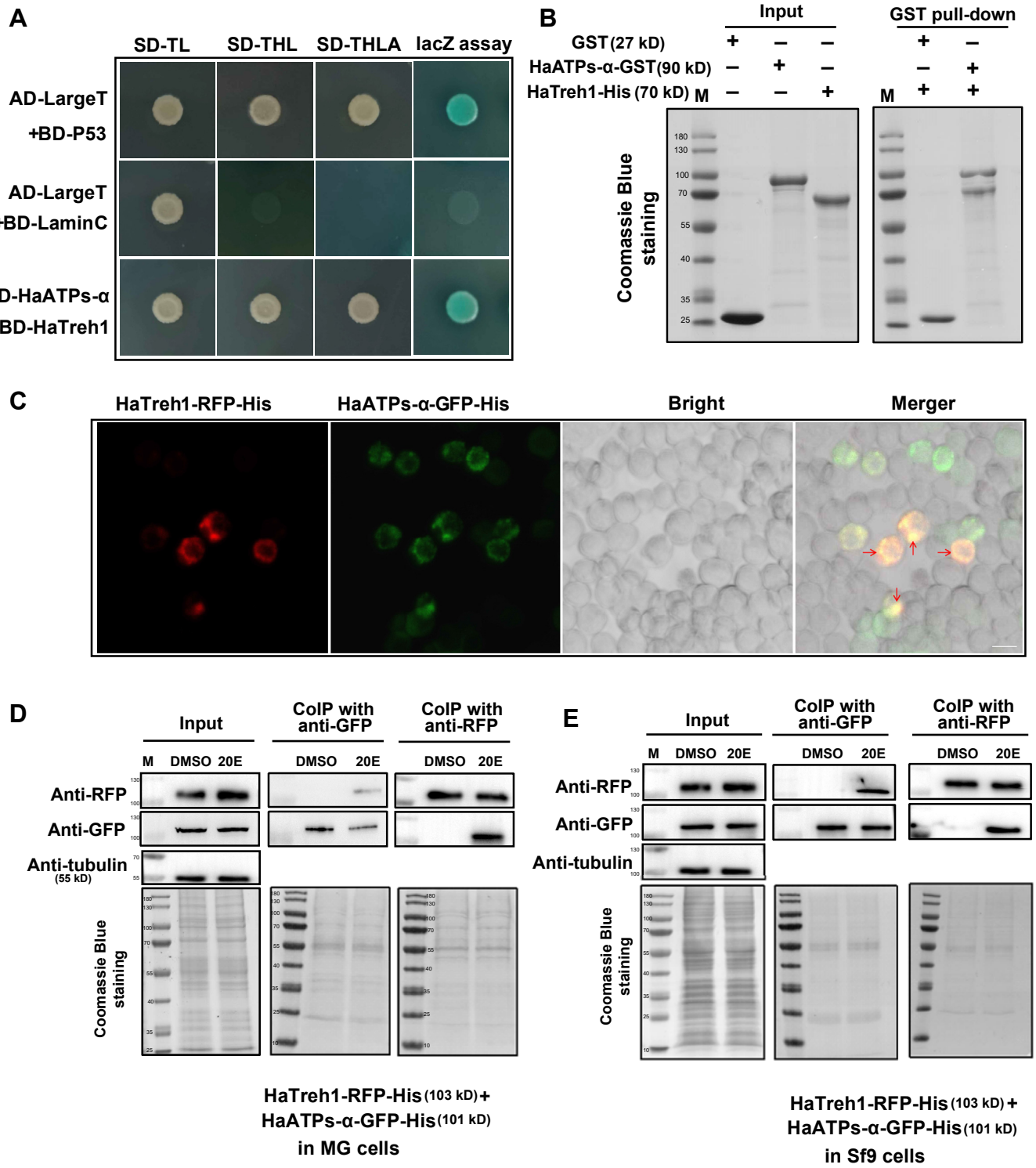

Figure 6. 20-hydroxyecdysone increased the binding of HaTreh1 and HaATPs-α. *A*, yeast two-hybrid experiment demonstrated the binding of BD-HaTreh1 with AD-HaATPs-α. AD-LargeT+BD-P53 was the positive control, and AD-LargeT+BD-LaminC was the negative control. *B*, glutathione-S-transferase pull-down assay proved the interaction between HaATPs-α and HaTreh1. M: protein marker. *C*, the colocalization of HaTreh1-RFP-His and HaATPs-α-GFP-His in midgut cells by LSM710. The bar was 10 μm. Merger was the overlap of *red* and *green*. The *arrow* indicates the overlapped *yellow*. *D*, Co-IP experiment proved that 20E (1 μM, 3 h) increased the combination between HaTreh1-RFP-His (103 kD) and HaATPs-α-GFP-His (101 kD) in midgut cells. M: protein marker. *E*, Co-IP experiment proved that 20E (1 μM, 3 h) increased the combination between HaTreh1-RFP-His (103 kD) and HaATPs-α-GFP-His (101 kD) in Sf9 cells. M: protein marker. 20E, 20-hydroxyecdysone; HaATPs-α, HaTreh1 with ATP synthase subunit alpha; RFP, Red fluorescent protein; Treh1, soluble Treh.

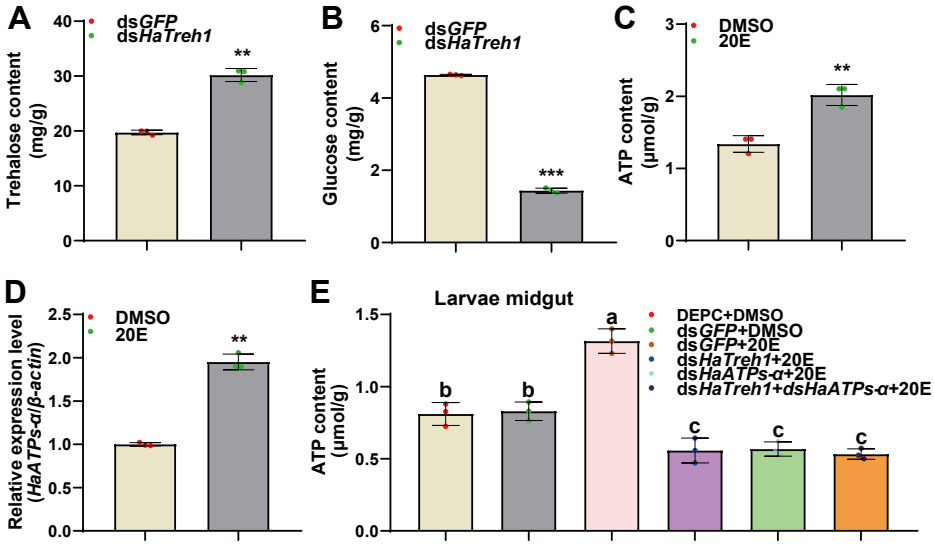

Figure 7. 20-hydroxyecdysone increased ATP production of larvae by HaTreh1 and HaATPs-α. *A* and *B*, the contents of trehalose (*A*) and glucose (*B*) in the midguts after injected with ds*GFP* (5 μg) or ds*HaTreh1* (5 μg) for 24 h. The error bars indicated the mean ± s.d. of three independent biological experiments and three technical repetitions. $^{**}p < 0.01$, $^{***}p < 0.001$, Student's *t* test. *C* and *D*, 20-hydroxyecdysone (1.2 μg, 1 μM, 6 h) increased the ATP content (*C*) and transcript level of *HaATPs*-α (*D*) in the midgut. The error bars indicated the mean ± s.d. of three independent biological experiments and three technical repetitions. $^{**}p < 0.01$, Student's *t* test. *E*, knockdown of *HaATPs*-α (5 μg, 5 μg, 24 h) or *HaTreh1* (5 μg, 5 μg, 24 h) decreased the induction of 20E (1.2 μg, 5 μl, 6 h) on ATP contents in the midgut. Diethyl pyrocarbonate (5 μl)+dimethyl sulfoxide (5 μl)-injected larvae were used as the blank control. The error bars indicated the mean ± s.d. of three independent biological experiments and three technical repetitions. *Different letters* indicate significant differences at $p < 0.05$ level by Tukey test. 20E, 20-hydroxyecdysone; HaATPs-α, HaTreh1 with ATP synthase subunit alpha; Treh1, soluble Treh.

that injected with ds*GFP* (3 μg) or ds*GFP* (3 μg) + 5 μl 20E (1.2 μg) were used as the control groups. Twelve larvae per group and three biological replicates were performed.

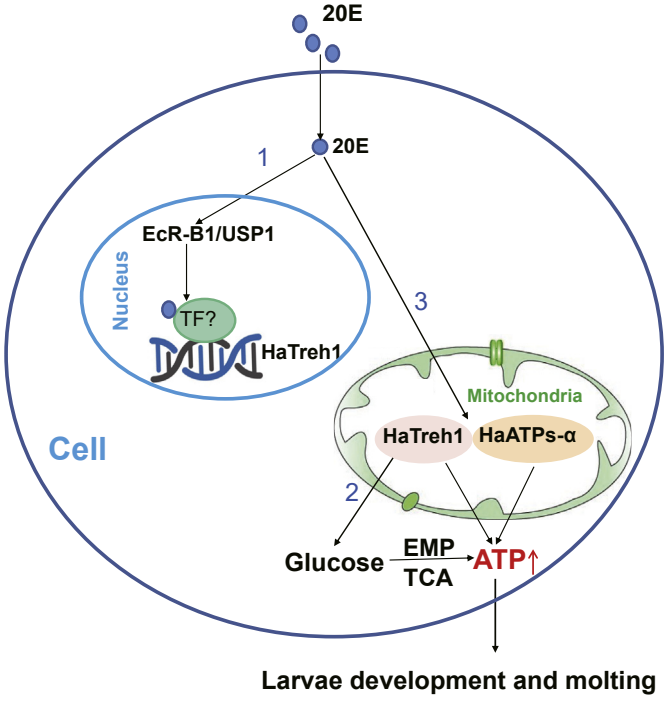

Figure 8. The function mechanism for HaTreh1 in the larvae. 1, 20-hydroxyecdysone upregulated the transcripts of *HaTreh1* by EcR-B1/USP1. 2 and 3, 20-hydroxyecdysone controlled the ATP production by increasing the interaction between HaTreh1 and HaATPs-α. EcR, ecdysone receptor; HaATPs-α, HaTreh1 with ATP synthase subunit alpha; Treh1, soluble Treh; USP, ultraspiracle protein.

Subcellular localization

The ORF sequence without the stop codon of *HaTreh1* was amplified by PCR with specific primers and then ligated with RFP-His-pIEx-4 vector to construct HaTreh1-RFP-His-pIEx-4 plasmid. HaTreh1-RFP-His-pIEx-4 was then transfected into MG cells with FuGENE HD Transfection Reagent (1 μg plasmid with 4 μl Transfection Reagent) (Promega, E2311) referred to previous description method (56). The cells transfected with RFP-His-pIEx-4 were used as the control. About 24 h after plasmids transfection, the fluorescence was observed and photographed at 24 h after transfection by LSM710 laser confocal (Zeiss).

After waiting 24 h, MG cells that transfected with HaTreh1-RFP-His-pIEx-4 plasmid were incubated with Mito-Tracker Green (C1048) (Beyotime) at 37 °C for 15 min (50 nM). The fluorescence images were photographed by LSM710 laser confocal (Zeiss).

Yeast two-hybrid assay

The ORF sequence of HaTreh1 without the stop codon were amplified by PCR with specific primers (Table S1) and then ligated with pGBKT7 plasmid to construct HaTreh1-pGBKT7. For Y2H library screening, HaTreh1-pGBKT7 containing AH109 cells mated with a *H. armigera* larvae Y2H library (constructed by Shanghai biogene biotechnology company) and then mated-culture were spread on the SD-TL, SD-THL, and SD-THLA plates and finally used for lacZ assay. For Y2H point to point assay, the ORF sequence of *HaATPs-α* (NCBI accession: XM_021337525.1) without the stop codon were amplified by PCR with specific primers (Table S1) and then ligated with pGADT7 plasmid to

construct HaATPs-α-pGADT7. AH109 competent cells were transformed with HaTreh1-pGBKT7 and HaATPs-α-pGADT7 as previous description (57) and then spotted on SD-TL, SD-TLH, SD-TLHA, and SD-TLHA+ x-α-gal plates. AH109 cells transfected with pGBKT7-P53 and pGADT7-largeT were used as positive control. AH109 cells transfected with pGBKT7-Laminc and pGADT7-largeT were used as the negative control.

Glutathione-S-transferase pull-down

The CDS of HaATPs-α and HaTreh1 were linked to pGEx-6P1 or pET30a plasmid to construct HaATPs-α-pGEx-6P1 and HaTreh1-pET30a, respectively. HaTreh1 with ATP synthase subunit alpha-GST, GST, and HaTreh1-His proteins were induced by IPTG and then purified by Glutathione SepHarose 4B (GE Healthcare) or Ni SepHarose six Fast Flow (GE Healthcare). The GST pull-down assay was performed referring to previous description (57). Briefly, 0.5 mg HaATPs-α-GST or GST purified proteins were incubated with 0.5 mg HaTreh1-His protein in the glutathione beads containing pull-down buffer at 4 °C for 4 h. Then, the beads were washed with washing buffer. Finally, the proteins were eluted from above beads with elution buffer. The protein samples were boiled and examined by SDS gel electrophoresis.

Coimmunoprecipitation

The ORF sequence of *HaATPs-a* was ligated with GFP-His-pIEx-4- vector to construct HaATPs-a-GFP-His-pIEx-4 plasmid. HaTreh1-RFP-His-pIEx-4 and HaATPs-a-GFP-His-pIEx-4 plasmids were cotransfected into MG cells (one Co-IP experiment with 7.2×10^6 cells and 4 μg of each plasmid), after 48 h, the cells were incubated with 20E (1 μM) for 3 h. Then, the cells were collected and lysed by Radio Immunoprecipitation Assay Lysis buffer (600 μl, containing protease inhibitor) on ice. Bicinchoninic acid protein assay kit (Solarbio) was used to determine the protein concentration. The input (60 μl) was took and the residual solution were divided into two equal parts. One part incubated with antibody according to the instructions of Biolinkedin GFP-Tag IP/Co-IP Kit (Biolinkedin) to purify the target GFP-tag proteins. Another part incubated with anti-RFP (Bioworld, MB2015) and rotated at 4 °C for 8 h and then incubated with Pierce Protein A/G Magnetic beads (ThermoFisher Scientific, 88802) for 2 h to purify the target RFP-tag proteins. Then, the protein samples were transferred into polyvinylidene fluoride membrane and detected using RFP or GFP antibodies by Western blotting. Protein samples were also detected by SDS-PAGE with Coomassie brilliant blue staining. The procedures of Co-IP experiments in the Sf9 cells were the same as above.

Measurement of trehalose and glucose contents after HaTreh1 knockdown

The sixth-instar larvae at 2 h after molting were selected. Larvae were injected with 5 μg ds*HaTreh1* or 5 μg ds*GFP* (about 5 μl), and then midguts were excised at 24 h after dsRNA injection.

Then, above treated midguts were homogenized and trehalose content was measured by the trehalose content detection kit (G0552W) (Greece Biotech) and the microplate reader (BioTek) with Anthrone colorimetry. Above dsRNA-injected midguts were homogenized and used for the glucose content detection by the kit (G0504W) (Greece Biotech) and the microplate reader (BioTek) with GOPOD Oxidase method. Six larvae per group and three biological replicates were performed.

Adenosine triphosphate content measurement

Samples with dsRNA-injection

The sixth-instar larvae at 2 h after molting were selected and there were six larvae in each group. Larvae were injected with 5 μg ds*GFP* (5 μl), 5 μg ds*HaTreh1*, 5 μg ds*ATPs-α*, or 5 μg ds*HaTreh1*+5 μg ds*ATPs-α*. After 24 h, dsRNA-injected larvae were injected with 20E (1.2 μg, 5 μl) or DMSO (5 μl) for 6 h. Diethyl pyrocarbonate (5 μl)+DMSO (5 μl)-injected larvae were used as the blank control. Then, the above treated larvae midguts were collected.

Samples under 20E treatment

The sixth-instar larvae at 2 h after molting were selected. Six larvae were used in each treatment. Larvae were injected with 5 μl 20E (1.2 μg, 1 μM) or 5 μl DMSO (diluted with 1× PBS to 1:10,000, the control group), and the midguts were excised at 24 h after injection.

Above collected-midguts were grounded and used for ATP content detection by the ATP content detection kit (BC0305) (Solarbio) and the microplate reader (BioTek). At least three biological replicates were used.

Data availability

All original data pertaining to this study will be made available upon request.

Supporting information—This article contains supporting information.

Acknowledgments—The work was supported by National Natural Science Foundation of China (31772536 and 31970472), National Science Fund of Henan Province for Distinguished Young Scholar (202300410191), Basic Research Project of the Key Scientific Research Projects of Universities in Henan Province (21zx013), Henan Agricultural Research System (Grant S2014-11-G06), Key Scientific Research Projects of Universities in Henan Province (22A210005), Henan Youth Talent Support Project (2022HYTP030), and Natural Science Youth Innovation Fund of Henan Agricultural University (KJCX2018A02 and KJCX2017A10).

Author contributions—Y. C., B. Z., M. D., J. W., and R. G. investigation; Z. G. and W. Z. methodology; W. Z. writing–original draft; S. A. writing–review and editing; S. A. funding acquisition.

Conflict of interest—The authors declare that they have no conflicts of interest with the contents of this article.

Abbreviations—The abbreviations used are: 20E, 20-hydroxyecdysone; ATPs, ATP synthase; ATPs-α, ATPs subunit alpha; CHS, chitin synthetase; Co-IP, coimmunoprecipitation; DMSO, dimethyl sulfoxide; EcR, ecdysone receptor; HaATPs-α, HaTreh1 with ATP synthase subunit alpha; MG cells, midgut cells; RFP, red fluorescent protein; Treh, trehalase; Treh1, soluble Treh; Treh2, membrane-bound Treh; USP, ultraspiracle protein; Y2H, yeast two-hybrid.

References

1. Elbein, A. D., Pan, Y. T., Pastuszak, I., and Carroll, D. (2003) New insights on trehalose: A multifunctional molecule. *Glycobiology* **13**, 17–27
2. Frison, M., Parrou, J. L., Guillaumot, D., Masquelier, D., François, J., Chaumont, F., and Batoko, H. (2007) The *Arabidopsis thaliana* trehalase is a plasma membrane-bound enzyme with extracellular activity. *FEBS Lett.* **581**, 4010–4016
3. Candy, D. J., and Kilby, B. A. (1961) The biosynthesis of trehalose in the *locust* fat body. *Biochem. J.* **78**, 531–536
4. Clegg, J. S., and Evans, D. R. (1961) Blood trehalose and flight metabolism in the *blowfly*. *Science* **134**, 54–55
5. Becker, A., Schlöder, P., Steele, J. E., and Wegener, G. (1996) The regulation of trehalose metabolism in insects. *Experientia* **52**, 433–439
6. Thompson Nelson, S. (2003) Trehalose – the insect 'blood' sugar. *Adv. Insect Physiol.* **31**, 205–285
7. Li, J., Li, S., Wang, D., and JI, R. (2014) Changes in the contents of stress resistant substances in *Gomphocerus sibiricus* (*Orthoptera: Acrididae*) under high temperature stress. *Acta Entomol. Sin.* **57**, 1155–1161
8. Valaitis, A. P., and Bowers, D. F. (1993) Purification and properties of the soluble midgut trehalase from the gypsy moth, *Lymantria dispar*. *Insect Biochem. Mol. Biol.* **23**, 599–606
9. Huang, J., Furusawa, T., Sadakane, K., and Sugimura, Y. (2006) Purification and properties of two types of soluble trehalases from embryonic larvae of the silkworm, *Bombyx mori*. *J. Insect Biotechnol. Sericology* **75**, 1–8
10. Silva, M. C., Ribeiro, A. F., Terra, W. R., and Ferreira, C. (2009) Sequencing of *Spodoptera frugiperda* midgut trehalases and demonstration of secretion of soluble trehalase by midgut columnar cells. *Insect Mol. Biol.* **18**, 769–784
11. Shimada, S., and Yamashita, O. (1979) Trehalose absorption related with trehalase in developing ovaries of the silkworm, *Bombyx mori*. *J. Comp. Physiol.* **131**, 333–339
12. Strang, R., and Clement, E. M. (1980) The relative importance of glucose and trehalose in the nutrition of the nervous system of the locust *Schistocerca americana gregaria*. *Insect Biochem. Mol. Biol.* **10**, 155–161
13. Takiguchi, M., Niimi, T., Su, Z. H., and Yaginuma, T. (1992) Trehalase from male accessory gland of an insect, *Tenebrio molitor*. cDNA sequencing and developmental profile of the gene expression. *Biochem. J.* **288**, 19–22
14. Wegener, G., Tschiedel, V., Schlöder, P., and Ando, O. (2003) The toxic and lethal effects of the trehalase inhibitor trehazolin in *locusts* are caused by hypoglycaemia. *J. Exp. Biol.* **206**, 1233–1240
15. Singtripop, T., Wanichacheewa, S., and Sakurai, S. (2000) Juvenile hormone-mediated termination of larval diapause in the bamboo borer, *Omphisa fuscidentalis*. *Insect Biochem. Mol. Biol.* **30**, 847–854
16. Ogiso, M., and Takahashi, S. Y. (1984) Trehalases from the male accessory glands of the *American Cockroach*: Developmental changes and the hormonal regulation of the enzymes. *Gen. Comp. Endocrinol.* **55**, 387–392
17. Mitsumasu, K., Azuma, M., Niimi, T., Yamashita, O., and Yaginuma, T. (2008) Changes in the expression of soluble and integral-membrane trehalases in the midgut during metamorphosis in *Bombyx mori*. *Zool. log. Sci.* **25**, 693–698
18. Kamei, Y., Hasegawa, Y., Niimi, T., Yamashita, O., and Yaginuma, T. (2011) Trehalase-2 protein contributes to trehalase activity enhanced by diapause hormone in developing ovaries of the silkworm, *Bombyx mori*. *J. Insect Physiol.* **57**, 608–613
19. Kh, S. D., and Keshan, B. (2021) The feeding status regulates the action of insulin and 20-hydroxyecdysone on haemolymph trehalose level in *Bombyx* larvae. *Comp. Biochem. Physiol. B Biochem. Mol. Biol.* **255**, 110579
20. Gilbert, L. I., Granger, N. A., and Roe, R. M. (2000) The juvenile hormones: Historical facts and speculations on future research directions. *Insect Biochem. Mol. Biol.* **30**, 617–644
21. Riddiford, L. M., Hiruma, K., Zhou, X., and Nelson, C. A. (2003) Insights into the molecular basis of the hormonal control of molting and metamorphosis from *Manduca sexta* and *Drosophila melanogaster*. *Insect Biochem. Mol. Biol.* **33**, 1327–1338
22. Oro, A. E., Mckeown, M., and Evans, R. M. (1990) Relationship between the product of the *Drosophila* ultraspiracle locus and the vertebrate retinoid X receptor. *Nature* **347**, 298–301
23. Kozlova, T., and Thummel, C. S. (2000) Steroid regulation of post-embryonic development and reproduction in *Drosophila*. *Trends Endocrinol. Metab.* **11**, 276–280
24. Thummel, C. S. (2002) Ecdysone-regulated puff genes 2000. *Insect Biochem. Mol. Biol.* **32**, 113–120
25. Li, T. R., and White, K. P. (2003) Tissue-specific gene expression and ecdysone-regulated genomic networks in *Drosophila*. *Dev. Cell* **5**, 59–72
26. Parthasarathy, R., and Palli, S. R. (2007) Developmental and hormonal regulation of midgut remodeling in a lepidopteran insect, *Heliothis virescens*. *Mech. Dev.* **124**, 23–34
27. Cai, M. J., Liu, W., He, H. J., Wang, J. X., and Zhao, X. F. (2012) Mod(mdg4) participates in hormonally regulated midgut programmed cell death during metamorphosis. *Apoptosis* **17**, 1327–1339
28. Denton, D., Chang, T. K., Nicolson, S., Shravage, B., Simin, R., Baehrecke, E. H., and Kumar, S. (2012) Relationship between growth arrest and autophagy in midgut programmed cell death in *Drosophila*. *Cell Death Differ.* **19**, 1299–1307
29. Lam, C. K., Zhao, W., Cai, W., Vafiadaki, E., Florea, S. M., Ren, X., Liu, Y., Robbins, N., Zhang, Z., Zhou, X., Jiang, M., Rubinstein, J., Jones, W. K., and Kranias, E. G. (2013) Novel role of HAX-1 in ischemic injury protection involvement of heat shock protein 90. *Circ. Res.* **112**, 79–89
30. Tang, B., Yang, M., Shen, Q., Xu, Y., Wang, H., and Wang, S. (2017) Suppressing the activity of trehalase with validamycin disrupts the trehalose and chitin biosynthesis pathways in the rice brown planthopper, *Nilaparvata lugens*. *Pestic. Biochem. Physiol.* **137**, 81–90
31. Tan, Y., Xiao, L., Sun, Y., Zhao, J., Bai, L., and Xiao, Y. (2014) Molecular characterization of soluble and membrane-bound trehalases in the cotton mirid bug, *Apolygus lucorum*. *Arch. Insect Biochem. Physiol.* **86**, 107–121
32. Li, Y. N., Liu, Y. B., Xie, X. Q., Zhang, J. N., and Li, W. L. (2020) The modulation of trehalose metabolism by 20-hydroxyecdysone in *Antheraea pernyi* (Lepidoptera: Saturniidae) during its diapause termination and post-termination period. *J. Insect Sci.* **20**, 1–5
33. Zhang, L., Qiu, L. Y., Yang, H. L., Wang, H. J., Zhou, M., Wang, S. G., and Tang, B. (2017) Study on the effect of wing bud chitin metabolism and its developmental network genes in the brown planthopper, *Nilaparvata lugens*, by knockdown of TRE gene. *Front. Physiol.* **8**, 750
34. Chen, J., Tang, B., Chen, H., Yao, Q., Huang, X., Chen, J., Zhang, D., and Zhang, W. (2010) Different functions of the insect soluble and membrane-bound trehalase genes in chitin biosynthesis revealed by RNA interference. *PLoS One* **5**, e10133
35. Gu, J., Ying, S., Zhang, C., Liu, Z., and Zhang, Y. (2009) Characterization of putative soluble and membrane-bound trehalases in a hemipteran insect, *Nilaparvata lugens*. *J. Insect Physiol.* **55**, 997–1002
36. Rolfe, D. F., Newman, J. M., Buckingham, J. A., Clark, M. G., and Brand, M. D. (1999) Contribution of mitochondrial proton leak to respiration rate in working skeletal muscle and liver and to SMR. *Am. J. Physiol.* **276**, C692–C699
37. Boyer, P. D. (1997) The ATP synthase - a splendid molecular machine. *Annu. Rev. Biochem.* **66**, 717–749
38. Capaldi, R. A., and Aggeler, R. (2002) Mechanism of the F(1)F(0)-type ATP synthase, a biological rotary motor. *Trends Biochem. Sci.* **27**, 154–160

39. Walker, J. E. (2013) The ATP synthase: The understood, the uncertain and the unknown. *Biochem. Soc. Trans.* **41**, 1–16
40. Kühlbrandt, W. (2019) Structure and mechanisms of F-type ATP synthases. *Annu. Rev. Biochem.* **88**, 515–549
41. Brown, S. V., Hosking, P., Li, J., and Williams, N. (2006) ATP synthase is responsible for maintaining mitochondrial membrane potential in bloodstream form *Trypanosoma brucei*. *Eukaryot. Cell* **5**, 45–53
42. Schnaufer, A., Clark-Walker, G. D., Steinberg, A. G., and Stuart, K. (2005) The F1-ATP synthase complex in bloodstream stage *trypanosomes* has an unusual and essential function. *EMBO J.* **24**, 4029–4040
43. Zíková, A., Schnaufer, A., Dalley, R. A., Panigrahi, A. K., and Stuart, K. D. (2009) The F(0)F(1)-ATP synthase complex contains novel subunits and is essential for procyclic *Trypanosoma brucei*. *PLoS Pathog.* **5**, e1000436
44. Kang, X. L., Zhang, J. Y., Wang, D., Zhao, Y. M., and Zhao, X. F. (2019) The steroid hormone 20-hydroxyecdysone binds to dopamine receptor to repress lepidopteran insect feeding and promote pupation. *PLoS Genet.* **15**, e1008331
45. Tang, B., Wei, P., Zhao, L., Shi, Z., Shen, Q., Yang, M., Xie, G., and Wang, S. (2016) Knockdown of five trehalase genes using RNA interference regulates the gene expression of the chitin biosynthesis pathway in *Tribolium castaneum*. *BMC Biotechnol.* **16**, 67
46. Shi, J. F., Xu, Q. Y., Sun, Q. K., Meng, Q. W., Mu, L. L., Guo, W. C., and Li, G. Q. (2016) Physiological roles of trehalose in *Leptinotarsa* larvae revealed by RNA interference of trehalose-6-phosphate synthase and trehalase genes. *Insect Biochem. Mol. Biol.* **77**, 52–68
47. Reed, W. D., and Sacktor, B. (1971) Localization of trehalase in flight muscle of the blowfly *Phormia regina*. *Arch. Biochem. Biophys.* **145**, 392–401
48. Chang, P. L., and Morrison, P. E. (1975) Histochemical localization of trehalase activity in dorsal flight muscle of the flesh fly *Sarcophaga bullata* with light and electron microscopy. *J. Histochem. Cytochem.* **23**, 800–807
49. Brandt, N. R., and Huber, R. E. (1979) The localization of honey bee thorax trehalase. *Can. J. Biochem.* **57**, 145–154
50. Hu, J., and Xia, Y. (2016) F1-ATP synthase α-subunit: A potential target for RNAi-mediated pest management of *Locusta migratoria manilensis*. *Pest Manag. Sci.* **72**, 1433–1439
51. Matassini, C., Parmeggiani, C., and Cardona, F. (2020) New frontiers on human safe insecticides and fungicides: An opinion on trehalase inhibitors. *Molecules* **25**, 3013
52. Zhao, X. C., Ma, B. W., Berg, B. G., Xie, G. Y., Tang, Q. B., and Guo, X. R. (2016) A global-wide search for sexual dimorphism of glomeruli in the antennal lobe of female and male *Helicoverpa armigera*. *Sci. Rep.* **6**, 35204
53. Wei, J., Liang, G., Wu, K., Gu, S., Guo, Y., Ni, X., and Li, X. (2018) Cytotoxicity and binding profiles of activated Cry1Ac and Cry2Ab to three insect cell lines. *Insect Sci.* **25**, 655–666
54. Chen, C. H., Pan, J., Di, Y. Q., Liu, W., Hou, L., Wang, J. X., and Zhao, X. F. (2017) Protein kinase C delta phosphorylates ecdysone receptor B1 to promote gene expression and apoptosis under 20-hydroxyecdysone regulation. *Proc. Natl. Acad. Sci. U. S. A.* **114**, E7121–E7130
55. Du, M., Zhang, S., Zhu, B., Yin, X., and An, S. (2012) Identification of a diacylglycerol acyltransferase 2 gene involved in pheromone biosynthesis activating neuropeptide stimulated pheromone production in *Bombyx mori*. *J. Insect Physiol.* **58**, 699–703
56. Blochlinger, K., and Diggelmann, H. (1984) Hygromycin B phosphotransferase as a selectable marker for DNA transfer experiments with higher eucaryotic cells. *Mol. Cell. Biol.* **4**, 2929–2931
57. Wang, K., Li, M. Q., Chang, Y. P., Zhang, B., Zhao, Q. Z., and Zhao, W. L. (2020) The basic helix-loop-helix transcription factor OsBLR1 regulates leaf angle in rice *via* brassinosteroid signalling. *Plant Mol. Biol.* **102**, 589–602